Desalination and Water Treatment
www.deswater.com

doi: 10.1080/19443994.2015.1137496

57 (2016) 23622–23632
October

Taylor & Francis
Taylor & Francis Group

Assessing dissolved organic matter in the Johannesburg-Sulfur autotrophic denitrification system using excitation—emission matrix fluorescence spectroscopy with a parallel factor analysis

Haibo Li[a,b,c], Beihai Zhou[a,*], Zhiyong Tian[b,c], Erdeng Du[d], Xiang Tu[b,c], Yonghui Song[b,c], Siyu Wang[b,c], Chen Sun[b,c]

[a]*Department of Environmental Engineering, School of Civil and Environmental Engineering, University of Science and Technology Beijing, Beijing 100083, China, Tel. +86 15652933695; email: lhb19850725@163.com (H. Li), Tel. +86 10 62334821; email: zhou_beihai@126.com (B. Zhou)*
[b]*State Key Laboratory of Environmental Criteria and Risk Assessment, Chinese Research Academy of Environmental Sciences, Beijing 100012, China, Tel. +86 18612834618; email: hkytzy2008@163.com (Z. Tian), Tel. +86 13811614067; email: tu_xiang@qq.com (X. Tu), Tel. +86 10 84924787; email: songyh@craes.org.cn (Y. Song), Tel. +86 13501010037; email: wangsiyu268@163.com (S. Wang), Tel. +86 18624321558; email: sunchen@craes.org.cn (C. Sun)*
[c]*Department of Urban Water Environmental Research, Chinese Research Academy of Environmental Sciences, Beijing 100012, China*
[d]*State Key Laboratory of Pollution Control an Resource Reuse, Tongji University, Shanghai 200092, China, Tel. +86 15810098590; email: 344969871@qq.com*

Received 25 June 2015; Accepted 17 December 2015

ABSTRACT

A novel system integrating Johannesburg (JHB) and sulfur autotrophic denitrification (SAD) process was proposed with the purpose of efficient removal of organic matter and nitrogen when treating low COD/TN ratio municipal wastewater. The characteristics and fate of dissolved organic matter in the Johannesburg-Sulfur autotrophic denitrification (JHB-SAD) system were investigated using excitation–emission matrix fluorescence spectroscopy with a parallel factor analysis. Three components were identified including tryptophan-like (component C_1), tyrosine-like (component C_2), and fulvic-like (component C_3) materials. The tyrosine-like and tryptophan-like materials, which were more abundant than fulvic-like materials, were the dominant components of the raw municipal wastewater in Shenyang North Wastewater Treatment Plant. In the JHB-SAD system, the tyrosine-like and tryptophan-like materials were more efficiently removed than the fulvic-like materials, and the removal efficiencies of the three components were 80.8% (tryptophan-like materials), 72.5% (tyrosine-like materials), and 33.4% (fulvic-like materials), respectively. Furthermore, the removal performance of the three components varied in the different zones of the JHB-SAD system. The tryptophan-like and fulvic-like materials were removed in the pre-anoxic, anaerobic, and aerobic zones. The tyrosine-like materials were mainly degraded in the anoxic and aerobic zones; then, they were released by the bacteria in the SAD reactor. In addition, the tryptophan-like materials had a very significant positive linear correlation with the concentrations of soluble chemical oxygen demand.

*Corresponding author.

Keywords: Johannesburg-Sulfur autotrophic denitrification (JHB-SAD); Dissolved organic matter (DOM); Excitation–emission matrix fluorescence (EEM); Parallel factor analysis (PARAFAC); Removal efficiency

1. Introduction

Excessive discharge of organic matter and nitrogen pollutants can result in the deterioration of water quality, eutrophication of water environments, and potential hazards to human health [1–3]. A stringent discharge standard (GB18918–2002) in China has been implemented to control the discharge of pollutants. Thus, efficient organic matter and nitrogen removals from municipal wastewater have become a challenge for wastewater treatment plants (WWTPs). Biological nutrient removal (BNR) systems, such as anaerobic/anoxic/aerobic (A^2/O) and anoxic/aerobic (A/O), are preferred and have been widely applied in innovative WWTPs due to their economic advantages compared with physicochemical technologies [3–6]. However, efficient nitrogen removal is typically unreliable because of the shortage of organic carbon [3,7,8]. Recently, a novel system integrating the Johannesburg (JHB) process and the sulfur autotrophic denitrification (SAD) process was developed to improve nitrogen removal from low COD/TN ratio municipal wastewaters [9]. The nitrogen removal efficiency of the JHB-SAD system reached 93.8% under a COD/TN ratio of 4–5. The JHB process combines the advantages of the anaerobic/anoxic/aerobic (A^2/O) process with the modified University of Cape Town (MUCT) process. An outstanding characteristic of the JHB process is the addition of a pre-anoxic zone prior to the A^2/O process to remove nitrates in return sludge. Due to limited organic carbon and inefficient heterotrophic denitrification, TN in the effluent of JHB was mainly composed of NO_3^--N with lower lever COD concentration. Based on the effluent characteristic of JHB process, SAD process was proposed to improve nitrogen removal performance. SAD bacteria can utilize sulfur as electron donor and nitrate as electron acceptor to carry out autotrophic denitrification. The stoichiometric equation of elemental-sulfur-utilizing autotrophic denitrification was described in Eq. (1) [10]:

$$1.06\,NO_3^- + 1.11\,S + 0.3\,CO_2 + 0.785\,H_2O = \Rightarrow 0.5\,N_2 + 1.11\,SO_4^{2-} + 1.16\,H^+ + 0.06\,C_5H_7O_2N \quad (1)$$

In this novel system, the JHB process mainly utilizes organic matter to remove nitrogen pollutants, but excellent nitrification in the JHB system is also necessary for enhanced nitrogen removal; thus, the SAD process, which utilizes sulfur as an electron donor, was integrated with the JHB process to further remove nitrate that was not removed due to carbon organic shortage. Therefore, JHB-SAD can achieve efficient nitrogen removal to treating the low COD/TN municipal wastewater.

The organic matter and nitrogen removal performances of the JHB-SAD system were excellent; however, a thorough analysis of the dissolved organic matter (DOM) was absent. DOM in municipal wastewater mainly includes protein, humus, grease, and surfactants [3]. Most of these compounds contain a fluorophore that emits a characteristic fluorescence when the excitation light is absorbed. The conventional monitoring indexes, such as chemical oxygen demand (COD), biochemical oxygen demand (BOD), and total organic carbon (TOC), only represent the total amount of organic matter, rather than distinguishing between the types of DOM. Further, the COD index is of limited use for assessing the characteristics and behaviors of DOM in the JHB-SAD system. Moreover, toxic DOM in raw municipal wastewater could result in low pollutant removal efficiency [11], and the DOM from the JHB-SAD system effluent could affect the receiving aqueous environment. Additionally, detailed information regarding DOM throughout the JHB-SAD system was scarce. Therefore, an insight into the characterization and assessment of DOM has become important for this novel JHB-SAD system.

Excitation–emission matrix (EEM) fluorescence spectroscopy has been commonly used to discriminate between types of DOM quickly and with a high sensitivity, which makes it an ideal method to characterize DOM [12–14]. The EEM fluorescence spectrum can be thought of as a fingerprint of samples that include key components in wastewater treatments. Additionally, mathematic methods such as parallel factor analysis (PARAFAC) have been used to interpret EEM [15–17]. Furthermore, EEM together with PARAFAC can provide a quantitative and qualitative characterization of DOM, and the spectral characteristics of individual fluorescence components when spectral overlapping of EEM fluorescence spectra are severe. Yang et al. [18] reported that the concentration and biodegradability

of organic matter could be estimated by EEM with PARAFAC. Yu et al. [19] reported that removal efficiency of types of DOM in wastewater treatment was assessed by EEM with PARAFAC. Therefore, The EEM with PARAFAC as potential monitoring technique may play an important role in accessing water quality of wastewater biotreatment system.

In this study, the characterization of DOM in the JHB-SAD system was investigated using EEM with PARAFAC. Based on the material balance, the fate of DOM was assessed using the maximum fluorescence intensity. The correlation between the DOM removal performance and the concentration of soluble chemical oxygen demand (SCOD) was also analyzed. These results provide useful information regarding the novel JHB-SAD system.

2. Experimental methods and materials

2.1. Experimental system and sample collection

A pilot-scale JHB-SAD system was installed to upgrade an original wastewater treatment system and to achieve effective organic matter and nitrogen removals from a low COD/TN ratio municipal wastewater. In order to reduce costs, the infrastructures of JHB process were established while considering existing infrastructures of original SDAO process (Shenyang Degremont Anoxic Oxic process). The anaerobic zone and pre-anoxic zone in JHB process were derived from the primary settler and the sludge recovery zone in SDAO process. The layout and a schematic diagram of the JHB-SAD system are provided in Fig. 1 and Supplementary information Fig. 1S, respectively. The JHB system consisted of pre-anoxic (PAN, volume of 0.83 m^3), anaerobic (ANA, volume of 1.61 m^3), anoxic (ANO, volume of 1.16 m^3), and aerobic zones (AE, volume of 2.77 m^3), in addition to a secondary settler (SES, working volume of 1.07 m^3). The diameter and the height of anaerobic zone were 1.10 and 1.85 m. The infrastructures of three circles with different diameter were embedded with each other and they were all 2.40 m in height. Center circle was pre-anoxic zone with 0.71 m in diameter; middle annulus was anoxic zone and its major diameter and minor diameter were 1.10 and 0.71 m, respectively; External annulus was aerobic zone and its major diameter and minor diameter were 1.70 and 1.10 m, respectively. The diameter and the height of secondary sedimentation tank were 1.00 and 2.35 m. Cylindrical section of secondary sedimentation tank was 1.23 m in height and circular cone section was 0.70 m in height. Due to the low COD/TN ratio, the SAD was added to improve the nitrogen removal performance. The secondary settler effluent from the JHB process was pumped into a SAD reactor. The height and inner diameter of the up-flow SAD reactor were 75 and 14 cm, respectively, and the packing height of the SAD reactor was 70 cm. The SAD reactor was filled with an equivalent diameter of 3–4 mm granular sulfur and 0.8–1.2 mm limestone (mass ratio 2:1), and the porosity of the reactor was 45.7%. The actual hydraulic retention time (AHRT) was 10 min.

The total inflow was maintained at 0.56 m^3/h during the JHB process, and the influent distribution ratio of the pre-anoxic and anaerobic zones were 30 and 70%, respectively. The nitrate recycling ratio (R) and sludge return ratio (r) were set at 200 and 100%, respectively, in the JHB process. The mixed liquor suspended solid (MLSS) was maintained at 2,500–2,700 mg/L. The sludge retention time (SRT) was maintained for 27–33 d by discharging the waste sludge. The dissolved oxygen (DO) concentration in the aerobic zone was controlled at 2.0–2.5 mg/L.

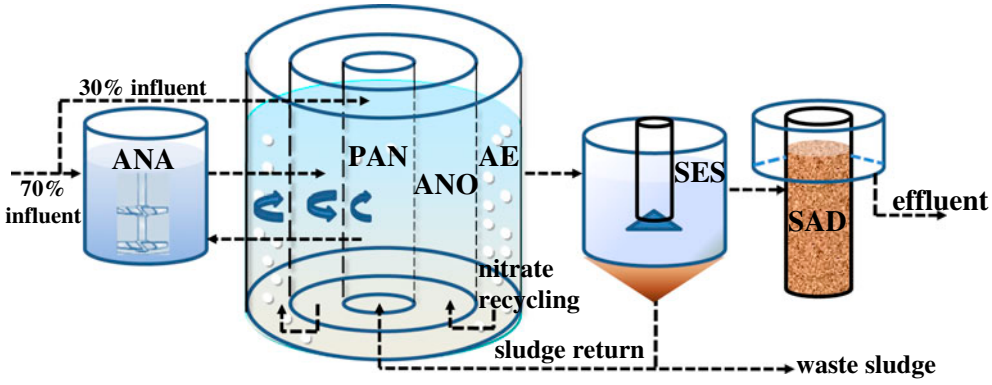

Fig. 1. Layout of the JHB-SAD system. PAN: pre-anoxic zone; ANA: anaerobic zone; ANO: anoxic zone; AE: aerobic zone; SES: secondary settler; SAD: sulfur autotrophic denitrification.

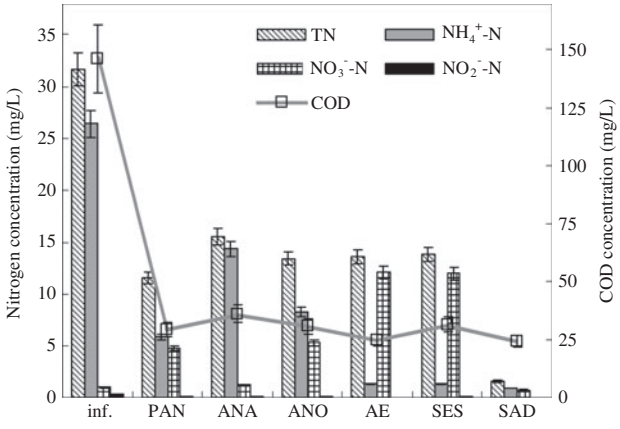

Fig. 2. Variations of the nitrogen and COD along the JHB-SAD system. inf: influent; PAN: pre-anoxic zone; ANA: anaerobic zone; ANO: anoxic zone; AE: aerobic zone; SES: secondary settler; SAD: sulfur autotrophic denitrification reactor.

The characteristics of the influent and pollutant removal performance of the JHB-SAD are described in Fig. 2. The influent temperature and operating temperature of JHB-SAD system was given in Supplementary information Fig. 2S.

The pilot-scale JHB-SAD system was conducted in Shenyang North WWTPs in Shenyang City, Liaoning Province, China. The raw municipal wastewater was collected from WWTP sewer line and pumped to pilot-scale JHB-SAD system. The water samples of JHB-SAD system were filtered using a glass fiber filter (nominal pore size 0.45 μm). The filtrate was stored in amber glass bottles at 4℃ until analysis, and all samples were analyzed within 48 h. The sampling times were 25 December 2013, 9 January 2014, and 20 January 2014, with the corresponding JHB-SAD operation phase of beginning, medium, and end.

2.2. Analytical methods

The SCOD was measured using a Lian-hua COD quick-analysis apparatus (Lian-hua Tech Co., Ltd, China).

The EEM of the samples was measured on a Hitachi Fluorescence Spectrophotometer (F-7000). The PMT voltage was set at 700 V, and both the excitation and emission slit widths were a 5-nm band pass with the scanning speed set at 2,400 nm min^{-1}. The EEM was measured with excitation wavelengths ranging from 260 to 550 nm and emission wavelengths ranging from 200 to 450 nm [13].

2.3. PARAFAC analysis method

Prior to the analysis, the Raman and Rayleigh scatter effects were removed by subtracting the pure water spectrogram from the sample spectrogram. The PARAFAC analysis was used to discriminate components from overlapping EEM fluorescence spectra data. All data were decomposed into a trilinear and a residual array using:

$$x_{ijk} = \sum_{f=1}^{F} a_{if}\, b_{jf}\, c_{kf} + e_{ijk} \tag{2}$$

where x_{ijk} was the fluorescence intensity of sample i at emission wavelength j and excitation wavelength k; F was the number of components; a_{if} was directly proportional to the relative intensity of component f in the sample i; b_{jf} and c_{kf} were scaled estimates of the fluorescence component f at emission wavelength j and excitation wavelength k, respectively; and e_{ijk} was the residual noise, which represents the variability not accounted for by the model [19]. Matlab software was used to calibrate and correct the data. The Domfluor toolbox 1.7 for Matlab was used to implement and validate the PARAFAC model [15]. In the PARAFAC analysis, independent components were identified and the maximum fluorescence intensity (F_{max}) of individual components was also obtained.

2.4. The calculation of pollutant removal efficiencies

The EEM with PARAFAC provided a characterization of the DOM in the JHB-SAD system. Based on the material balance, individual component removal efficiencies within the JHB-SAD system were calculated using Eqs. (3) through (8).

$$\text{Pre-anoxic zone: } S_{PAN} = \frac{30\% \cdot C_{inf} + r \cdot C_{SES} + (30\% + r) \cdot C_{PAN}}{C_{inf}} \tag{3}$$

$$\text{Anaerobic zone: } S_{ANA} = \frac{(30\% + r) \cdot C_{PAN} + 70\% \cdot C_{inf} - (1 + r) \cdot C_{ANA}}{C_{inf}} \quad (4)$$

$$\text{Anoxic zone: } S_{ANO} = \frac{(1 + r) \cdot C_{ANA} + R \cdot C_{AE} - (1 + r + R) \cdot C_{ANO}}{C_{inf}} \quad (5)$$

$$\text{Aerobic zone: } S_{AE} = \frac{(1 + r + R) \cdot C_{ANO} - (1 + r + R) \cdot C_{AE}}{C_{inf}} \quad (6)$$

$$\text{Secondary settler: } S_{SES} = \frac{(1 + r) \cdot C_{AE} - (1 + r) \cdot C_{SES}}{C_{inf}} \quad (7)$$

$$\text{SAD reactor: } S_{SAD} = \frac{C_{SES} - C_{SAD}}{C_{inf}} \quad (8)$$

where S_{PAN}, S_{ANA}, S_{ANO}, S_{AE}, S_{SES}, and S_{SAD} were individual component removal efficiencies in the pre-anoxic zone, anaerobic zone, anoxic zone, aerobic zone, secondary settler, and SAD reactor, respectively; the C_{inf}, C_{PAN}, C_{ANA}, C_{ANO}, C_{AE}, C_{SES}, and C_{SAD} represented the F_{max} of the individual components in the influent, pre-anoxic zone, anaerobic zone, anoxic zone, aerobic zone, secondary settler, and SAD reactor, respectively; 30 and 70% denoted the influent distribution ratio of the pre-anoxic and anaerobic zones, respectively; and R and r were the nitrate recycling and sludge return ratios, respectively. Eqs. (3) through (8) were used to calculate the DOM component removal efficiencies of the different zones (Fig. 5(b)).

2.5. Correlation analysis between the SCOD and F_{max} of the individual components

To study the correlation between the F_{max} of the individual components and the SCOD, we utilized the following linear regression model (9):

$$Y = kX + C_0 \quad (8)$$

where Y was the SCOD concentration; X was the independent variable and represented the F_{max} of the individual components; and k and C_0 were constant values. Eq. (9) was used to assess the correlation between the SCOD and F_{max} of the individual components (Fig. 6). In addition, the correlation between the SCOD and F_{max} of the individual components were also investigated by calculating Pearson correlation coefficients using SPSS Statistics 19 software (IBM, USA).

3. Results and discussion

3.1. EEM spectra characteristic and PARAFAC analysis of JHB-SAD system

The EEM spectra of the raw municipal wastewater and the JHB-SAD system were presented in Fig. 3 and Supplementary information Figs. S3 and S4. There were five fluorescence peaks (B_1, B_2, T_1, T_2, and C) identified in the influent. Peak B_1 (Ex/Em = 225–230/310 nm) and peak B_2 (Ex/Em = 275–280/305–310 nm) were attributed to the protein fluorescence of the tyrosine-like materials [19,20]. Peak T_1 (Ex/Em = 225–235/345–350 nm) and peak T_2 (Ex/Em = 280/350–355 nm) were related to the protein fluorescence of the tryptophan-like materials [19]. A shoulder peak C (Ex/Em = 315–320/405–410 nm) was found and described for the visible fulvic-like materials [19]. In

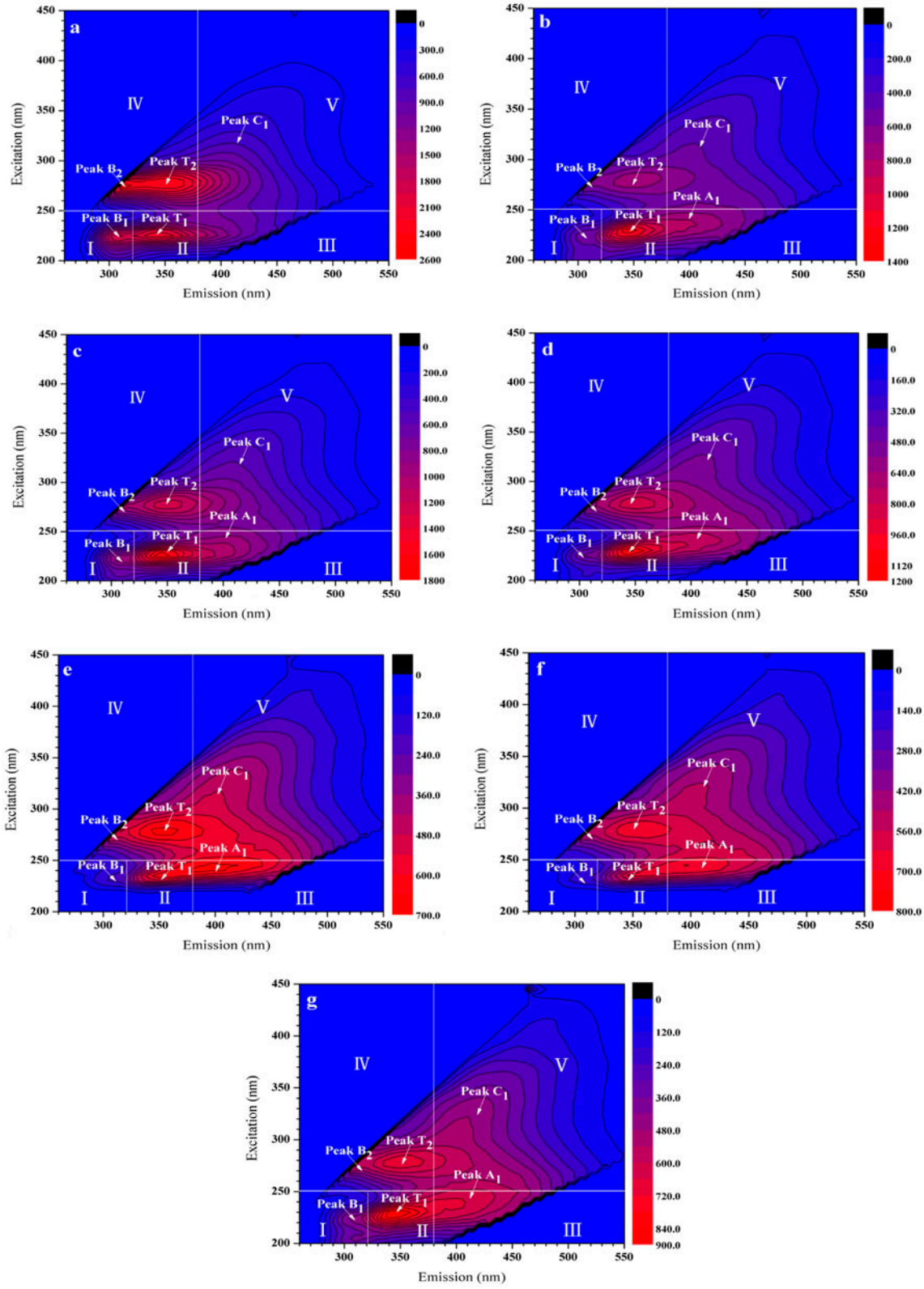

Fig. 3. Variations of the EEM spectra along the JHB-SAD system on 9 January 2014: (a) influent; (b) pre-anoxic zone; (c) anaerobic zone; (d) anoxic zone; (e) aerobic zone; (f) secondary settler effluent; (g) SAD reactor effluent.

addition, a new peak A (Ex/Em = 240–245 nm/395–405 nm) was detected in the JHB-SAD system and related to the UV-fulvic-like materials [21]. The fluorescence intensity of peak A changed little in the JHB-SAD system.

Compared with peaks A and C, the fluorescence intensities of peaks B_1, B_2, T_1, and T_2 were significantly decreased throughout the JHB system. This indicated that the protein-like materials were decomposing in the JHB process. Moreover, the JHB process was inefficient at removing the fulvic-like materials that were refractory biodegradable organic compounds. However, the fluorescence intensity of peaks B_1 and T_1 were increased in the SAD reactor, which could be related to the metabolism of SAD bacteria. Microorganisms can produce multiple types of compounds, such as proteins, coenzymes, and humus [22–24]. The microbial metabolites related to peaks B_1 and T_1 could not be effectively decomposed by the SAD bacteria compared with decomposition by heterotrophic micro-organisms in the JHB process. This is because the SAD bacteria are autotrophic micro-organisms and are inefficient at removing organic matter.

Throughout the JHB-SAD system, the fluorescence peak intensity ratios of B_2/B_1 and T_2/T_1 were mutative (Table 1). The intensity ratios of B_2/B_1 and T_2/T_1 revealed a constitution of protein-like materials [25]. Table 1 shows that the peak intensity ratios of B_2/B_1 were increased in the aerobic zone, whereas T_2/T_1 was decreased in the non-aerobic zone and then increased in the aerobic zone. This result indicated that the protein-like materials related to the peaks of B_1 tended to be removed in the aerobic zone, whereas the protein-like materials related to the peaks of T_2 tended to be decomposed in the non-aerobic zone. In the SAD process, the peak intensity ratios of B_2/B_1 and T_2/T_1 were decreased. This indicated that the protein-like materials, related to the peaks of B_1 and T_1, were mainly microbial metabolites produced by the SAD bacteria.

PARAFAC modeling was used to separate the overlapping EEM spectra and to analyze the independent fluorescence components. Three components (C_1, C_2, and C_3) were identified by PARAFAC (Fig. 4). The components, C_1, C_2, and C_3, all exhibited primary and secondary peaks located at Ex/Em of 225 and 280/345 nm (component C_1), Ex/Em of 230/305 and 345 nm (component C_2) and Ex/Em of 245 and 310/420 nm (component C_3). Based on the position of the peak, the composition of the components could be determined according to previously reported categories [15,19]; component C_1 was related to a tryptophan-like material, component C_2 was related to a tyrosine-like material, and component C_3 was determined to be a fulvic-like material.

The maximum fluorescence intensities (F_{max}) of the individual components were also obtained using PARAFAC. F_{max} was related to the concentration of different components [19]. Fig. 5(a) shows the F_{max} of the fluorescence components during the wastewater treatment. The average F_{max} of components C_1 (F_{max} of 2,588 au) and C_2 (F_{max} of 1,834 au) were higher than that of component C_3 (F_{max} of 879.1 au) in the influent. The EEM spectra characteristic and PARAFAC analysis showed that the tyrosine-like and tryptophan-like materials were the dominant fluorescence components in the raw municipal wastewater of Shenyang North WWTPs where the JHB-SAD system located at, which is consistent with the results of previous studies [26–28]. Those two protein materials are mainly derived from washing water, food residue, excrement, and other proteins [29]. Fulvic-like materials were also found in the wastewater, and these originated in residual humus in drinking water or microbial metabolites in sewer lines [22,23,30].

3.2. The calculation of fluorescence component removal efficiencies

The fate of the fluorescence components were tracked using their F_{max} values in the JHB-SAD system. The F_{max} and removal efficiencies of components C_1, C_2, and C_3 along the JHB-SAD system are shown in Fig. 5. Throughout the JHB-SAD system, components C_1 and C_2 were significantly decreased compared with component C_3, and the average F_{max} in the system effluent were 497.0 au (component C_1), 503.7 au (component C_2), and 585.2 au (component C_3). The three component removal efficiencies in the JHB-SAD system were 80.8% (component C_1), 72.5% (component C_2) and 33.4% (component C_3).

Table 1
Variations of the fluorescence peak intensity ratios along the JHB-SAD system

	Inf.	PAN	ANA	ANO	AE	SES	SAD
B_2/B_1	1.19 ± 0.08	1.56 ± 0.33	1.02 ± 0.13	1.47 ± 0.11	2.96 ± 0.28	3.03 ± 0.21	1.93 ± 0.81
T_2/T_1	0.98 ± 0.10	0.74 ± 0.12	0.72 ± 0.04	0.85 ± 0.10	1.02 ± 0.10	1.06 ± 0.14	0.81 ± 0.27

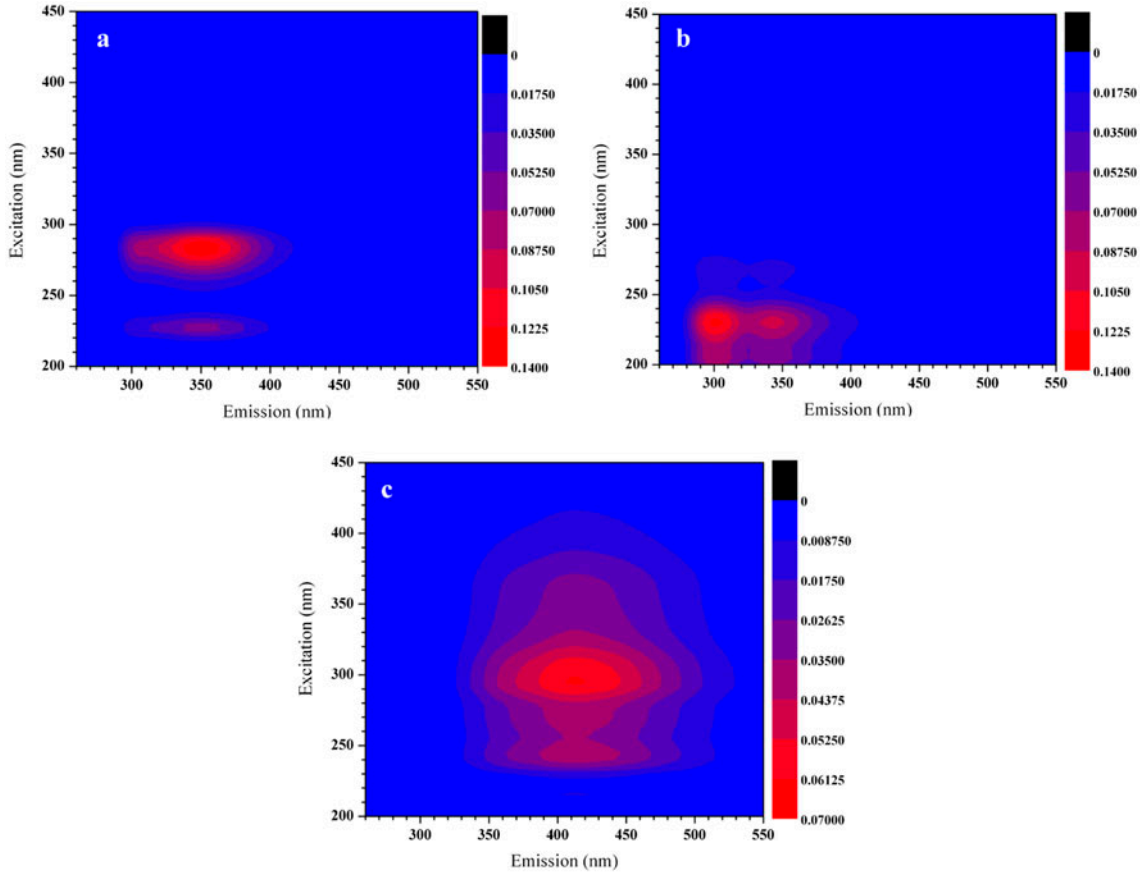

Fig. 4. The three components of the JHB-SAD system decomposed using the PARAFAC approach: (a) component C_1; (b) component C_2; (c) component C_3.

As shown in Fig. 5(b), component C_1 was mainly degraded in the pre-anoxic, anaerobic, and aerobic zones, and the corresponding removal efficiencies were 19.1, 38.6, and 21.6%, respectively. The anoxic zone and the SAD reactor were inefficient at removing component C_1. Component C_2 removal efficiencies in the anoxic and aerobic zones were 25.1 and 65.3%, respectively, which indicated that component C_2 was mainly removed in the anoxic and aerobic zones. The removal efficiency of component C_3 was lower than for components C_1 and C_2 in the JHB-SAD system. Component C_3 was mainly removed in the pre-anoxic (9.92%), anaerobic (7.55%), and aerobic zones (17.1%). In contrast, the F_{max} of components C_2 and C_3 increased in the SAD process and anoxic zones, respectively, indicating that microbial metabolites in the SAD process and anoxic zone were associated with the tyrosine-like (component C_2) and fulvic-like (component C_3) materials, respectively. The results suggested the following. First, protein-like materials (component C_1 and C_2) were effectively removed in the JHB-SAD system. Second, bacteria in the pre-anoxic and anaerobic zones tended to degrade tryptophan-like materials (component C_1). Bacteria in the anoxic zone tended to remove tyrosine-like materials (component C_2). At the same time, nitrate was removed in pre-anoxic, anaerobic, and anoxic zone via heterotrophic denitrification as shown in Fig. 2. It indicated that tryptophan-like materials (component C_1) severed as electron donor for heterotrophic denitrification reaction in pre-anoxic and anaerobic zone, and tyrosine-like materials (component C_2) were utilized as electron donor by heterotrophic denitrification bacteria in anoxic zone. Third, bacteria in the aerobic zone were able to remove both tryptophan-like and tyrosine-like materials (components C_1 and C_2), and pollutants could be further decomposed by aerobic micro-organism to lower concentration level comparing to non-aeration micro-organism in JHB process. Fourth, tyrosine-like materials (component C_2) were generated and released by the metabolism of SAD bacteria (this result was

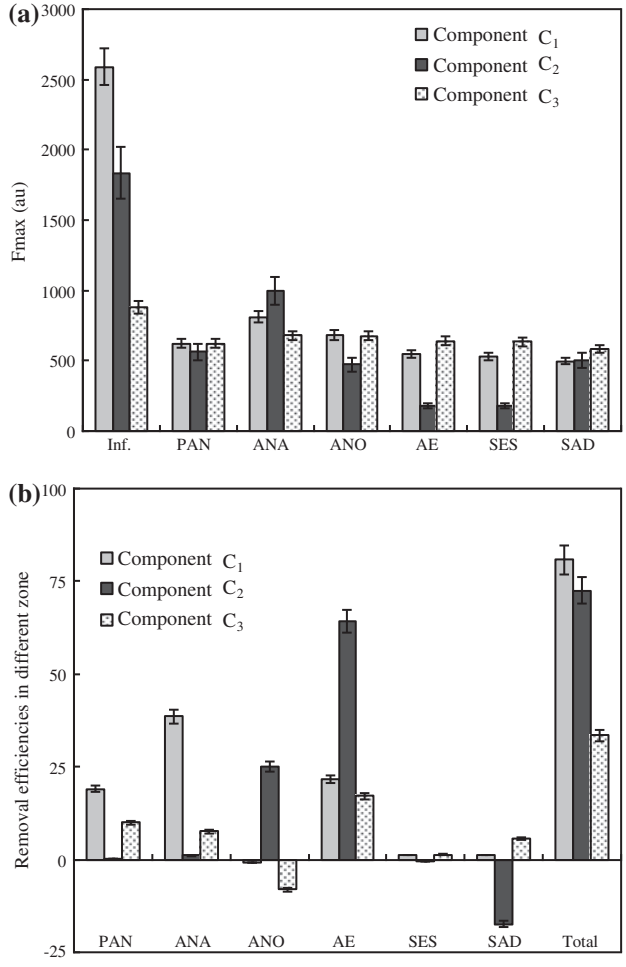

Fig. 5. F_{max} values (a) and removal efficiencies (b) of the PARAFAC components along the JHB-SAD system.

consistent with that reported in Section 3.1 of this study). Fulvic-like materials (component C_3) were released in the anoxic zone and then a part of component C_3 was removed in the aerobic zone. Fifth, the JHB-SAD system was inefficient at removing fulvic-like materials (component C_3) compared with the removal of protein-like materials.

3.3. Correlation between the SCOD and F_{max} of the individual components

The SCOD concentrations were fitted to the F_{max} of the individual components using the linear regression model: $Y = kX + C_0$ (Fig. 6). The F_{max} of component C_1 revealed the most positive linear correlation with the concentrations of SCOD (which were SCOD = 0.0283 C_1 + 8.356, the correlation coefficient R^2 = 0.9687). In contrast, the correlation between the SCOD and F_{max} of components C_2 and C_3

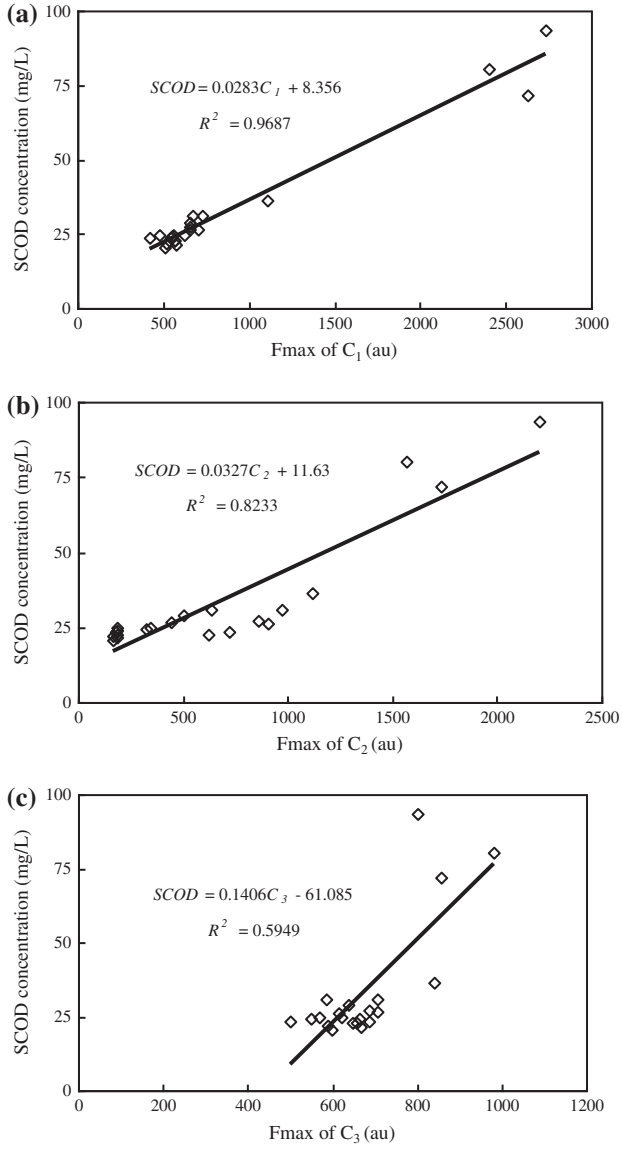

Fig. 6. Correlation between the SCOD concentration and the F_{max} of components: C_1 (a); C_2 (b); C_3 (c).

was SCOD = 0.0327 C_2 + 11.63 (R^2 = 0.8233) and SCOD = 0.1406 C_3 – 61.085 (R^2 = 0.5949), respectively. On the other hand, the correlation between SCOD and F_{max} of the individual components was further accessed by calculating Person correlation coefficients. The results showed that the Person correlation coefficients between SCOD and F_{max} of components C_1, C_2, and C_3 were 0.984, 0.907, and 0.771, respectively. Therefore, the order of correlation between the SCOD concentration and F_{max} of the individual components was F_{max} of component C_1 > F_{max} of component C_2 > F_{max} of component C_3. The results indicated that component C_1, related to tryptophan-like materials, can be used as an indicator of SCOD in the JHB-SAD system.

4. Conclusions

The main conclusions of this study are as follows: (1) tryptophan-like and tyrosine-like materials were the dominant fluorescence components in the raw municipal wastewater and were more efficiently removed than the fulvic-like materials in the JHB-SAD system; (2) bacteria in the non-aerobic zone of the JHB process tended to remove protein-like materials, and bacteria in the aerobic zone of the JHB process were able to remove multiple DOMs; (3) the tyrosine-like materials were released by bacteria in the SAD reactor; and (4) a significant positive linear correlation was found between the tryptophan-like materials and SCOD.

Supplementary material

The supplementary material for this paper is available online at http://dx.doi.10.1080/19443994.2015.1137496.

List of symbols

x_{ijk}	—	the fluorescence intensity of sample i at the emission wavelength j and excitation wavelength k
F	—	the number of components
a_{if}	—	the relative intensity proportion of component f in the simple I
b_{if} and c_{kf}	—	the scaled estimates of the fluorescence component f at the emission wavelength j and excitation wavelength k
e_{ijk}	—	the residual noise
S_{PAN}, S_{ANA}, S_{ANO}, S_{AE}, S_{SES}, and S_{SAD}	—	the individual component removal efficiencies in the pre-anoxic zone, anaerobic zone, anoxic zone, aerobic zone, secondary settler, and SAD reactor, respectively
C_{inf}, C_{PAN}, C_{ANA}, C_{ANO}, C_{AE}, C_{SES}, and C_{SAD}	—	the F_{max} of the individual components in the influent, pre-anoxic zone, anaerobic zone, anoxic zone, aerobic zone, secondary settler, and SAD reactor, respectively

Acknowledgments

This work was financially supported by the Major Science and Technology Program for Water Pollution Control and Treatment of China (2012ZX07202-005 & 2013ZX07202-010).

References

[1] H. Bothe, S.J. Ferguson, W.E. Newton, Biology of the Nitrogen Cycle, Elsevier, Netherlands, 2007.
[2] X. Li, H. Chen, Q. Yang, D. Wang, K. Luo, G. Zeng, Biological nutrient removal in a sequencing batch reactor operated as oxic/anoxic/extended-idle regime, Chemosphere 105 (2014) 75–81.
[3] M. Henze, M.C.M. Van Loosdrecht, G.A. Ekama, D. Brdjanovic, Biological Wastewater Treatment: Principles, Modelling and Design, IWA Publishing, London, 2008.
[4] B. Xie, J. Zuo, L. Gan, F. Liu, K. Wang, Cation exchange resin supported nanoscale zero-valent iron for removal of phosphorus in rainwater runoff, Front. Environ. Sci. Eng. 8 (2014) 463–470.
[5] S. Ge, Y. Zhu, C. Lu, S. Wang, Y. Peng, Full-scale demonstration of step feed concept for improving an anaerobic/anoxic/aerobic nutrient removal process, Bioresour. Technol. 120 (2012) 305–313.
[6] Y. Liu, H. Shi, W. Li, Y. Hou, M. He, Inhibition of chemical dose in biological phosphorus and nitrogen removal in simultaneous chemical precipitation for phosphorus removal, Bioresour. Technol. 102 (2011) 4008–4012.
[7] G. Cao, S. Wang, Y. Peng, Z. Miao, Biological nutrient removal by applying modified four step-feed technology to treat weak wastewater, Bioresour. Technol. 128 (2013) 604–611.
[8] Y. Chen, B. Li, L. Ye, Y. Peng, The combined effects of COD/N ratio and nitrate recycling ratio on nitrogen and phosphorus removal in anaerobic/anoxic/aerobic (A^2/O)-biological aerated filter (BAF) systems, Biochem. Eng. J. 93 (2015) 235–242.
[9] H. Li, B. Zhou, Z. Tian, Y. Song, L. Xiang, S. Wang, C. Sun, Efficient biological nitrogen removal by Johannesburg-Sulfur autotrophic denitrification from low COD/TN ratio municipal wastewater at low temperature, Environ. Earth Sci. 73 (2015) 5027–5035.
[10] A. Koenig, L.H. Liu, Kinetic model of autotrophic denitrification in sulphur packed-bed reactors, Water Res. 35 (2001) 1969–1978.
[11] H.S. Ou, C.H. Wei, C.-H. Mo, H.-Z. Wu, Y. Ren, Novel insights into anoxic/aerobic1/aerobic2 biological fluidized-bed system for coke wastewater treatment by fluorescence excitation–emission matrix spectra coupled with parallel factor analysis, Chemosphere 113 (2014) 158–164.
[12] E. Cohen, G.J. Levy, M. Borisover, Fluorescent components of organic matter in wastewater: Efficacy and selectivity of the water treatment, Water Res. 55 (2014) 323–334.
[13] J. Wei, Y. Song, X. Tu, L. Zhao, E. Zhi, Pretreatment of dry-spun acrylic fiber manufacturing wastewater by Fenton process: Optimization, kinetics and mechanisms, Chem. Eng. J. 218 (2013) 319–326.
[14] X.S. He, B.-D. Xi, R.T. Gao, L. Wang, Y. Ma, D.Y. Cui, W.B. Tan, Using fluorescence spectroscopy coupled with chemometric analysis to investigate the origin, composition, and dynamics of dissolved organic

matter in leachate-polluted groundwater, Environ. Sci. Pollut. Res. 22 (2015) 8499–8506.
[15] C.A. Stedmon, R. Bro, Characterizing dissolved organic matter fluorescence with parallel factor analysis: A tutorial, Limnol. Oceanogr. Methods 6 (2008) 572–579.
[16] X.S. He, B.-D. Xi, H.W. Pan, X. Li, D. Li, D.Y. Cui, W.B. Tang, Y. Yuan, Characterizing the heavy metal-complexing potential of fluorescent water-extractable organic matter from composted municipal solid wastes using fluorescence excitation–emission matrix spectra coupled with parallel factor analysis, Environ. Sci. Pollut. Res. 21 (2014) 7973–7984.
[17] X.S. He, B.-D. Xi, X. Li, H.W. Pan, D. An, S.G. Bai, D. Li, D.Y. Cui, Fluorescence excitation-emission matrix spectra coupled with parallel factor and regional integration analysis to characterize organic matter humification, Chemosphere 93 (2013) 2208–2215.
[18] L. Yang, H.S. Shin, J. Hur, Estimating the concentration and biodegradability of organic matter in 22 wastewater treatment plants using fluorescence excitation emission matrices and parallel factor analysis, Sensors 14 (2014) 1771–1786.
[19] H. Yu, Y. Song, X. Tu, E. Du, R. Liu, J. Peng, Assessing removal efficiency of dissolved organic matter in wastewater treatment using fluorescence excitation emission matrices with parallel factor analysis and second derivative synchronous fluorescence, Bioresour. Technol. 144 (2013) 595–601.
[20] P.G. Coble, Characterization of marine and terrestrial DOM in seawater using excitation-emission matrix spectroscopy, Mar. Chem. 51 (1996) 325–346.
[21] F.C. Wu, E. Tanoue, Isolation and partial characterization of dissolved copper-complexing ligands in streamwater, Environ. Sci. Technol. 35 (2001) 3646–3652.
[22] D.J. Barker, D.C. Stuckey, A review of soluble microbial products (SMP) in wastewater treatment systems, Water Res. 33 (1999) 3063–3082.
[23] B. Ni, F. Fang, W. Xie, M. Sun, G. Sheng, W. Li, H. Yu, Characterization of extracellular polymeric substances produced by mixed microorganisms in activated sludge with gel-permeating chromatography, excitation-emission matrix fluorescence spectroscopy measurement and kinetic modeling, Water Res. 43 (2009) 1350–1358.
[24] W.H. Li, G.P. Sheng, X.W. Liu, H.Q. Yu, Characterizing the extracellular and intracellular fluorescent products of activated sludge in a sequencing batch reactor, Water Res. 42 (2008) 3173–3181.
[25] J. Wu, S. Cui, C. Xie, Z. Cao, M. Chen, Y. Lv, Fluorescence fingerprint transformation of municipal wastewater caused by aerobic treatment, Spectrosc. Spectral Anal. 31 (2011) 3302–3306 (in Chinese).
[26] U.K. Ahmad, Z. Ujang, Z. Yusop, T.L. Fong, Fluorescence technique for the characterization of natural organic matter in river water, Water Sci. Technol 46 (2002) 117–125.
[27] N. Hudson, A. Baker, D. Reynolds, Fluorescence analysis of dissolved organic matter in natural, waste and polluted waters—A review, River Res. Appl. 23 (2007) 631–649.
[28] N. Hudson, A. Baker, D. Ward, D.M. Reynolds, C. Brunsdon, C. Carliell-Marquet, S. Browning, Can fluorescence spectrometry be used as a surrogate for the biochemical oxygen demand (BOD) test in water quality assessment? An example from South West England, Sci. Total Environ. 391 (2008) 149–158.
[29] M. Chen, J. Wu, Y. Lv, Q. Chen, Fluorescence properties of municipal wastewater, Acta Optica Sin. 28 (2008) 578–582 (in Chinese).
[30] S.A. Baghoth, S.K. Sharma, G.L. Amy, Tracking natural organic matter (NOM) in a drinking water treatment plant using fluorescence excitation–emission matrices and PARAFAC, Water Res. 45 (2011) 797–809.